Physica Scripta. Vol. T59, 286–293, 1995

Quantum Effects in Measurements on Trapped Ions*

D. J. Wineland, J. C. Bergquist, J. J. Bollinger and W. M. Itano

National Institute of Standards and Technology, Division 847.10, 325 Broadway, Boulder, CO 80303, U.S.A.

Received September 30, 1994; accepted January 20, 1995

Abstract

Quantum mechanical effects which are manifested in measurements on trapped atomic ions are reviewed. Observation of these effects is facilitated by the long storage times of a fixed number of laser-cooled ions and by high detection sensitivities, primarily through the observation of scattered laser light. We discuss the observation of quantum jumps and the application of quantum jumps to measurement of atomic ion lifetimes and spectra, detection of antibunching of light, the quantum Zeno effect and quantum projection noise. Experiments which detect nonclassical features of fluorescent light from single or a few trapped ions are briefly reviewed. Finally, we discuss experiments which reveal quantum effects in the motion of trapped ions. We briefly describe possible future extensions for each of these topics.

1. Introduction

In this paper we review how quantum effects are manifested in measurements on one ion or small numbers of ions and indicate how these quantum effects can be used to advantage in current and planned experiments. Historically, the relationship between experimental measurements and the theory of quantum mechanics often centered on the description and interpretation of thought experiments involving single particles. Not so long ago, Schrödinger dismissed some of the conclusions drawn from these thought experiments by writing [1] "... we never experiment with just one electron or atom or (small) molecule. In thought experiments we sometimes assume we do; this invariably entails ridiculous consequences." However with ion traps, it has become possible to do (repeated) measurements on single electrons [2, 3] and atoms [4, 5]; some of these experiments have forced a re-examination of the relationship between experiment and theory.

Here, we briefly highlight the connection between measurement and quantum theory; however, we will avoid issues of interpretation of quantum mechanics, such as the relationship of the wave function to single-particle experiments. We will use the idea of "collapse of the wave function" and "projection" when these are consistent with the experimental results and give a simple interpretation of the results. However, this is not meant to imply that we favor, say, the Copenhagen interpretation over the statistical-ensemble interpretation [6]. This pragmatic approach is discussed more fully in Ref. [7].

For most of the topics included here, there is nothing special, in principle, about atomic ions versus neutral atoms. However, in actual experiments, because of the overall charge of atomic ions, traps for ions are typically much stronger than for neutral atoms. This has enabled long confinement times and good localization, allowing either single or a few atomic ions to be detected with high sensitivity. In some experiments, these properties have facilitated the observation of quantum mechanical effects in the measurements.

This paper is not intended to give a comprehensive treatment of the topics included. Rather, when appropriate, we will refer to more complete reviews.

2. Quantum jumps

The notion of quantum jumps in atomic systems goes back as far as Bohr's model of the atom and the idea that transitions between atomic states take place instantaneously [8]. Interest in the subject of quantum jumps was rekindled recently by experiments using small numbers of ions in traps. Although many features of quantum jumps were apparent in the work by Van Dyck, Dehmelt, and their collaborators on single electrons [3], interest appeared to peak later, stimulated by Dehmelt's proposal for detection of transitions by means of "electron shelving" [9], the ability to observe single ions in traps [4, 5], and a theoretical paper by Cook and Kimble [10]. The subject has been covered in detail by review articles [11–13].

Dehmelt [9] considered the situation illustrated in Fig. 1. Suppose we are interested in detecting a transition between levels 1 and 2 in a single atom. We assume the decay rate $1/\tau_2$ from state 2 back to state 1 is very slow. Now assume level 1 can also be connected to a third level, level 3, by a strongly allowed (typically, electric-dipole) transition. We assume level 3 has a very short lifetime τ_3 and that the $1 \rightarrow 3$ transition is driven with near saturating intensity. Dehmelt noted that if we observe the fluorescence from level 3, we can sensitively detect transitions from level 1 to 2 because absorption of one photon on the $1 \rightarrow 2$ transition causes the cessation of about τ_2/τ_3 fluorescent photons from level 3. Dehmelt called this amplification by "electron shelving" [9] – the transition is detected by "shelving" the atomic electron in level 2 and the number of photons is amplified by a factor of $A_Q \simeq \tau_2/\tau_3$; that is, the absorption of one $1 \rightarrow 2$ photon results in a change of $\simeq \tau_2/\tau_3$ scattered photons on the $1 \rightarrow 2$ transition.

The cases where τ_2/τ_3 is very large have significant practical advantage for spectroscopy. Typically the net collection efficiency η for detecting scattered photons, including limited solid angle and photon detector quantum efficiency, is less than 1%. Therefore, if we detected the $1 \rightarrow 2$ transition by observing $2 \rightarrow 1$ fluorescent photons, for example,

* Contribution of NIST; not subject to U.S. copyright.

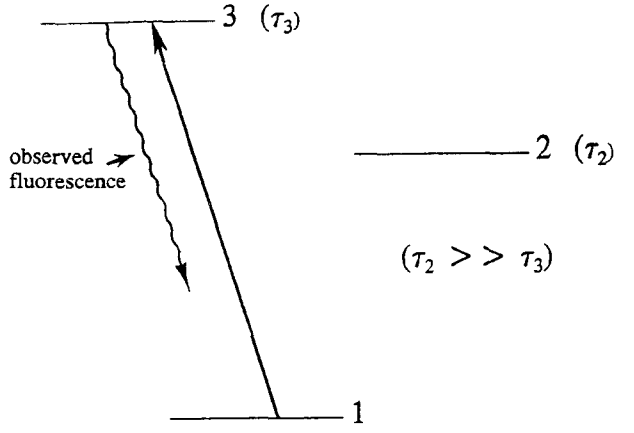

Fig. 1. Three-level system relevant for discussions of detection by "electron shelving" quantum amplification and quantum jumps. Level 1 is assumed stable. Levels 2 and 3 decay radiatively to level 1 with lifetimes τ_2 and τ_3 respectively where $\tau_3 \ll \tau_2$. We assume the $1 \rightarrow 3$ transition is driven near saturating intensity and the $3 \rightarrow 1$ fluorescent photons are detected. Atoms can be transferred to level 2 by, for example, the absorption of a single photon of frequency $\omega_{12} \simeq (E_2 - E_1)/\hbar$. This causes interruption of approximately τ_2/τ_3 fluorescent $3 \rightarrow 1$ photons and indicates a transition of the atom to level 2. Because each photon causing a $1 \rightarrow 2$ transition results in a change of τ_2/τ_3 fluorescent $3 \rightarrow 1$ photons, a quantum amplification of $A_Q \simeq \tau_2/\tau_3$ is achieved.

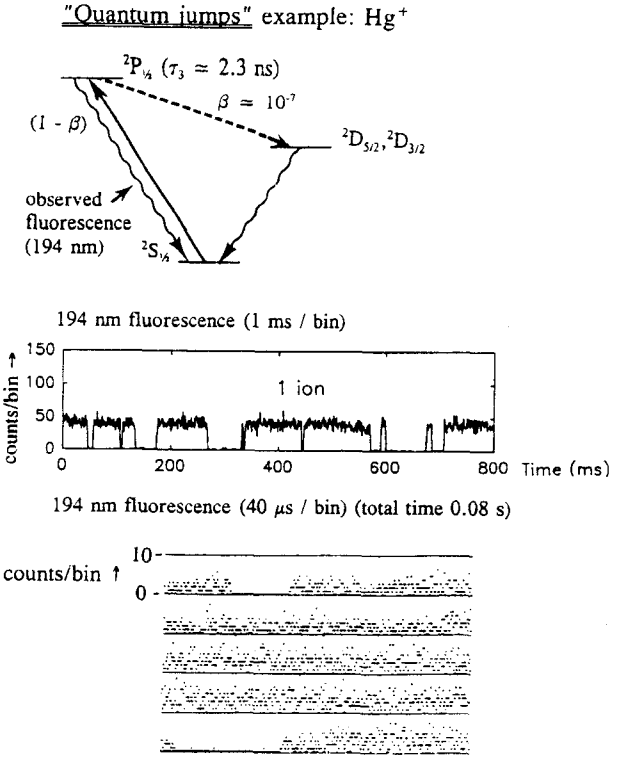

Fig. 2. Quantum jumps observed in the experiments of Refs [17, 19]. In these experiments on single ^{198}Hg ions, the $^2S_{1/2} \rightarrow ^2P_{1/2}$ transition is driven with narrowband radiation near 194 nm. With small branching ratio ($\beta \simeq 10^{-7}$) the ion decays from the $^2P_{1/2}$ state to the metastable $^2D_{3/2}$ level which can subsequently decay to the $^2D_{5/2}$ state or back to the ground state. When the ion is in one of the ^2D states, the 194 nm fluorescence ceases for about 0.01 to 0.1 s. The sudden cessation of the fluorescence (the sudden transition from steady fluorescence to no fluorescence as illustrated by the data) indicates the "jump" of the ion from the $^2P_{1/2}$ state to the $^2D_{3/2}$ state. The sudden reappearance of fluorescence indicates the jump of the ion from one of the ^2D states to the $^2S_{1/2}$ state. For times shorter than the inverse of the mean $3 \rightarrow 1$ fluorescence rate, we cannot say which level the ion is in. The bottom part of the figure shows a continuous recording of the fluorescence (arranged in five rows) for a total time of 80 ms. In this trace, the time sample (bin) width is 40 μs. The vertical scale shows quantization due to the detection of single $3 \rightarrow 1$ fluorescent photons.

we would miss detecting many $1 \rightarrow 2$ transitions, and the signal-to-noise ratio in the experiment would be correspondingly reduced. However, if we instead look for a change in the $3 \rightarrow 1$ fluorescent photons, we can detect all $1 \rightarrow 2$ transitions provided $\tau_2/\tau_3 \gg \eta^{-1}$. (In a high-precision experiment designed to measure the $1 \rightarrow 2$ transition frequency, we usually want to alternately apply the $1 \rightarrow 2$ radiation and the $1 \rightarrow 3$ radiation in order to avoid the shifts of level 1 caused by the $1 \rightarrow 3$ radiation.)

Cook and Kimble [10] considered the situation where the $1 \rightarrow 2$ and $1 \rightarrow 3$ radiations were applied simultaneously. Initially, most people agreed that when the $1 \rightarrow 2$ radiation was resonant, the average fluorescence on the $1 \rightarrow 3$ transition would decrease. However there was discussion whether $3 \rightarrow 1$ fluorescence would decrease uniformly or whether it would switch from "on" to "off" as Cook and Kimble had assumed – the latter picture consistent with the idea that the atom would "jump" between levels 1 and 2. This second picture became the accepted one. This was perhaps most clearly explained in the discussion of Cohen-Tannoudji and Dalibard, who calculated the distribution function for the delays between successive $3 \rightarrow 1$ fluorescent photons [14]. If the $1 \rightarrow 3$ transition is driven with near saturation intensity, the mean time between emitted fluorescent $3 \rightarrow 1$ photons is approximately τ_3 if the atom is not in level 2. If no photons are emitted after several times τ_3, the probability that the atom would be found in state 2 rapidly approaches unity, and we say that the atom has jumped to level 2. For times shorter than τ_3 we cannot say which level the atom is in. (In a real experiment, we cannot say which level the atom is in for durations less than the mean time between detected photons.) The quantum jumps were graphically illustrated in experiments on single atomic ions which showed bistability in the $3 \rightarrow 1$ fluorescence [15–17]. Some data for the experiments of Ref. 17 are shown in Fig. 2. The jumps could also be seen on ensembles of N ions as steps between $N + 1$ fluorescence levels. A number of additional experimental and theoretical analyses were published which are summarized in the reviews [11–13].

3. Applications of quantum jumps and Dehmelt's electron shelving amplification

3.1. *Lifetimes*

Referring to Fig. 1, assume that only $1 \rightarrow 3$ radiation is applied to the atom. Now suppose that level 3 can decay to level 2 with a probability β much smaller than the decay back to level 1 as indicated in the example in Fig. 2. This decay is revealed by the fact that the fluorescence switches off for a (mean) time τ_2 (Fig. 2); that is, the atom makes a quantum jump from level 3 to level 2. From the statistics of the off times, τ_2 is determined. In some sense, this method of measuring lifetimes takes advantage of the ergodic theorem where the lifetimes can be measured in single measurements on an ensemble of N atoms or by making N sequential measurements on an identically prepared atom. Single atom lifetimes have been determined for $Ba^+(5d^2D_{5/2})$ [15, 16, 18],

Hg^+ ($6s^2D_{3/2,5/2}$) [19], $Sr^+(^2D_{5/2})$ [20, 21], $Ca^+(^2D_{5/2})$ [22], and $In^+(^3P_0)$ [23] from an analysis of the quantum jumps. General methods for lifetime measurements using trapped ions have been reviewed by Church at this conference and in Ref. [24].

3.2. *Antibunching*

Following the discussion of Section 3.1, we note that the single ion emitting photons of frequency ω_{32} on the $3 \rightarrow 2$ transition can be viewed as a source of antibunched light at this frequency [25]. In an antibunched light source, two photons from the source cannot be emitted at the same time. Here, photon antibunching simply results from the fact that if the ion emits a $3 \rightarrow 2$ photon, it must first pass through states 1 and 3 before emitting a subsequent $3 \rightarrow 2$ photon. The photons emitted on the $3 \rightarrow 2$ transition also show sub-Poissan statistics. (See Section 4.2 below.)

3.3. *Quantum Zeno effect*

The quantum Zeno effect can be defined as the inhibition of transitions due to frequent measurements. It can be explained in the following way. Suppose a quantum system is initially in an eigenstate $|\phi\rangle$, so we write its wave function at time $t = 0$ as $|\psi(0)\rangle = |\phi\rangle$. We now subject the system to a perturbation H where, for simplicity, we assume H is time independent (when H is time dependent, we can usually transform to a frame where it is time independent). At time t, we have $|\psi(t)\rangle = \exp[-i(H/\hbar)t]|\phi\rangle$. If we make a measurement on the system at time t, the probability of the system remaining in the state $|\phi\rangle$ is equal to $P_\phi = |\langle\phi|\psi(t)\rangle|^2$. For short enough times, we find $P_\phi \simeq 1 - [(\Delta H)^2/\hbar^2]t^2$, where $(\Delta H)^2 \equiv \langle\phi|H^2|\phi\rangle - \langle\phi|H|\phi\rangle^2$. Now if, instead, we make n measurements on the system at times t/n, $2t/n$, $3t/n$, ..., t, the probability of finding the system in state $|\phi\rangle$ after time t is $P_\phi(n) \simeq \{1 - [(\Delta H)^2/\hbar^2](t/n)^2\}^n$. As $n \rightarrow \infty$, $P_\phi(n) \rightarrow 1$. Therefore if the system is measured often enough, the transition is prevented.

The quantum Zeno effect can be demonstrated by the system shown in Fig. 1 [26]. Suppose that the $3 \rightarrow 2$ and $2 \rightarrow 1$ decays are negligible [$\beta \rightarrow 0$ (Fig. 2), $\tau_2 \rightarrow \infty$]. Assume the atom starts in the level 1 (eigenstate $|1\rangle$) and the $1 \rightarrow 3$ radiation is off. We now apply radiation (the perturbation) which drives the atom from state 1 to 2. This perturbation is time dependent, but in a particular interaction picture and using the rotating wave approximation, it is time independent (in this case, $|1\rangle$ and $|2\rangle$ are not stationary states). The measurements in the experiment can be made by applying short pulses of $1 \rightarrow 3$ radiation. For each of these pulses, if $3 \rightarrow 1$ fluorescence is induced, we can think of the atom being projected into state 1. If no fluorescence is induced we can think of the atom being projected into state 2. We do not have to observe the fluorescence with an actual detector; it is only necessary that it could, in principle, be observed. Such an experiment was performed on $^9Be^+$ ions in a Penning trap [27] confirming the basic features of the quantum Zeno effect. In Ref. [27], each time the measurement pulse was applied the atom would scatter many photons ($\simeq 70$) if the atom was projected to state 1. It would be interesting to extend these measurements to the regime of incomplete measurements; that is where the number of scattered photons would be on the order of 1 or less for each measurement pulse [28].

The experiment of Ref. [27] was a demonstration of the Zeno effect on an induced transition; that is, we induced the $1 \rightarrow 2$ transitions with external radiation. It would be interesting to observe the Zeno effect on radiative decay, that is, inhibit radiative decay through frequent measurement. In general however, the bandwidth of the vacuum fields (the perturbation H) is so large that the time over which $1 - P_\phi \propto t^2$ is too short to be experimentally accessible [13, 27]. This experimental problem might be overcome by placing the atom in a cavity, thereby reducing the bandwidth of the (vacuum) radiation and extending the time over which $1 - P_\phi \propto t^2$ [27].

3.4. *Spectroscopy*

We have already noted the importance of quantum amplification ($A_Q = \tau_2/\tau_3$) for spectroscopy in the introduction to Section 2. In early experiments on Mg^+, values of $A_Q \simeq 10^6$ were realized [29]. In these experiments, τ_3 was the (allowed) decay time from the $^2P_{3/2}$ state, and τ_2 was caused by optical pumping from level 2 to level 1 by the $1 \rightarrow 3$ laser radiation. The high value of A_Q allowed the detection of weak absorption lines but, in that experiment, performed on many (10^3–10^4) ions, other sources of noise prevented the observation of the discrete fluorescence changes from the quantum jumps. This situation changed with the first quantum jump experiments on single (or a few) ions [15–17]. These experiments showed that transitions could be detected with 100% efficiency; this capability was first applied in atomic ion spectroscopy to detect the optical quadrupole $^2S_{1/2} \rightarrow {}^2D_{5/2}$ transition in a single $^{198}Hg^+$ ion [30]. In this experiment, the optical quadrupole transition (the $1 \rightarrow 2$ transition of Fig. 1, $\lambda \simeq 282$ nm) was first driven with radiation near the rest frequency. This radiation was then turned off, and radiation approximately resonant with the strongly allowed $^2S_{1/2} \rightarrow {}^2P_{1/2}$ transition (the $1 \rightarrow 3$ transition in Fig. 1, $\lambda \simeq 194$ nm) was applied. When the $^2P_{1/2} \rightarrow {}^2S_{1/2}$ fluorescence was absent, it could be assumed the ion had made the transition to the $^2D_{5/2}$ state. In this way the spectrum in Fig. 3 was achieved. This technique has been used in other single ion experiments to detect optical transitions in Ba^+ [31, 32] and Sr^+ [33, 34].

3.4.1. *Quantum projection-noise limit in spectroscopy.* Although transitions can be detected with 100% efficiency, the signal-to-noise ratio in spectroscopy is limited by fundamental quantum fluctuations. To see this, we examine the method described in Section 3.4 in closer detail. We have assumed we detect atomic transitions by observing changes in atomic state population (as opposed to observing, say, changes in the transmitted radiation). In general, we first localize an ensemble of N identical atoms (ions) in a trap, where N remains fixed throughout the experiments. We initially prepare each of the atoms in the same internal eigenstate, which we take to be state $|1\rangle$. We then apply (classical) radiation, which we will call the clock radiation, to the atoms. The clock radiation has a frequency that drives the atoms from eigenstate $|1\rangle$ to eigenstate $|2\rangle$. After application of this radiation, an atom is, in general, in a coherent superposition state $c_1|1\rangle + c_2|2\rangle$, where $|c_1|^2 + |c_2|^2 = 1$. Here, we have assumed that relaxation of states 1 and 2 is negligible; this is often a good approx-

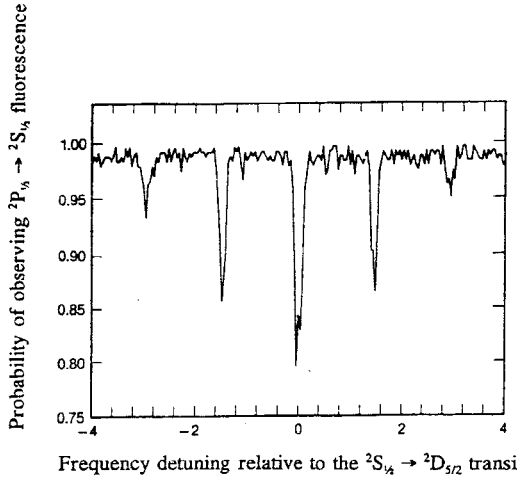

Fig. 3. Spectrum of the electric-quadrupole-allowed $5d^{10}6s\,^2S_{1/2}(m_J = -\frac{1}{2}) \rightarrow 5d^9 6s^2\,^2D_{5/2}(m_J = \frac{1}{2})$ transition in a single, laser-cooled $^{198}Hg^+$ ion taken using Dehmelt's method of quantum-amplification detection by electron shelving. On the horizontal axis is plotted the relative detuning from line center in frequency units at 282 nm. On the vertical axis is plotted the probability that the fluorescence from the $6s\,^2S_{1/2}$–$6p\,^2P_{1/2}$ first resonance transition, excited by laser radiation at 194 nm, is on. The $S \rightarrow D$ transition and $S \rightarrow P$ transition are probed sequentially in order to avoid light shifts and broadening of the $S \rightarrow D$ transition. Clearly resolved are the recoilless absorption resonance or "carrier" (the central feature) and the Doppler-shift-induced frequency-modulation sidebands due to the residual secular motion of the laser-cooled ion. Each point is the average of 230 measurement cycles. (From Ref. [30]).

imation for stored atomic ions. We then detect the number of atoms in state $|1\rangle$ by looking for the presence of $3 \rightarrow 1$ fluorescence when we apply the $1 \rightarrow 3$ radiation). In the detection process, we will find each atom to be in either eigenstate $|1\rangle$ or $|2\rangle$; that is, the measurement can be thought of as projecting the atom into one of these states. If we perform this preparation, irradiation, and detection many times, on average we will detect $N_1 = |c_1|^2 N$ atoms to be in state $|1\rangle$. However, unless $|c_1| = 1$ or 0, the number of atoms found in state $|1\rangle$ will fluctuate from measurement to measurement. We call these fluctuations "projection noise" [7]. They are given by $\Delta N_1 = [N|c_1|^2(1 - |c_1|^2)]^{1/2}$. In the experiments of Ref. [30], the noise was dominated by the noise in the laser which drove the $1 \rightarrow 2$ transition. This "technical" noise masked the projection noise. Recently, in related experiments [7], we have reduced all sources of technical noise so that the signal-to-noise ratio is limited by projection noise. In those experiments, ΔN_1 was given by the expression above. The ability to clearly see the projection noise was enabled by detecting a fixed number of atomic ions with high efficiency using Dehmelt's electron shelving detection scheme.

Projection noise is the fundamental limiting noise in spectroscopic experiments which detect transitions by monitoring changes in population on a fixed number of particles. However, if the fields which drive the clock transition are quantum fields or, if we assume that they are quantum fields and that we detect the clock transition by observing changes in the transmitted clock radiation, then we must account for the additional quantum noise inherent in the clock radiation.

3.4.2. *Improvements using quantum mechanically correlated atoms.* In the method of spectroscopy described in the previous section, we assumed all of the atoms are initially prepared in the $|1\rangle$ state. This is an uncorrelated state for all atoms because the total wave function can be written as a direct product of the individual states,

$$\Psi(t=0) = \prod_{i=1}^{N} |1\rangle_i .$$

Suppose that after application of the clock radiation, the signal is given by detecting an operator $\tilde{O}$ which yields the number of atoms remaining in state $|1\rangle$ ($\tilde{O} \equiv \tilde{N}_1$). We can characterize the sensitivity of the measurement to changes in the frequency ω of the applied clock radiation by the parameter $|\Delta\omega| \equiv \Delta\tilde{O}/|\partial\langle\tilde{O}\rangle/\partial\omega|$ where $(\Delta\tilde{O})^2 \equiv \langle\tilde{O}^2\rangle - \langle\tilde{O}\rangle^2$. For a given number of atoms N and a given interaction time in which the clock radiation is applied, we want $|\Delta\omega|$ to be as small as possible. We can show [35] that $\Delta\omega$, limited only by the quantum fluctuations in the measurement process (the projection noise), is proportional to $N^{-1/2}$. This was the case realized in the experiments reported in Ref. [7]. However, if the ensemble of atoms is initially prepared in particular correlated states

$$\left(\Psi(0) \neq \prod_{i=1}^{N} |1\rangle_i\right),$$

the precision of a transition frequency measurement can improve nearly as N^{-1} ($\Delta\omega$ approximately proportional to N^{-1}) [35].

To explain the basic idea, first recall that since the spectroscopy of any two-level system is equivalent to that of a spin-$\frac{1}{2}$, the spectroscopy of N two-level systems can be thought of as the spectroscopy of a composite spin

$$\boldsymbol{J} = \sum_i \boldsymbol{s}_i ,$$

where $s_i = \frac{1}{2}$. Second, assume a particular form of spectroscopy commonly used in experiments: the separated oscillatory field technique invented by Ramsey. In the Ramsey technique, the ensemble is initially prepared in a state with mean spin vector $\langle\boldsymbol{J}\rangle$ oriented along the z-axis. After application of the two separated (in time) fields, the population of one of the two levels ($|1\rangle$ or $|m_s = -\frac{1}{2}\rangle$ assumed here) for each atom is measured. This is equivalent to measuring J_z since in this case, $\tilde{O} = \tilde{N}_1 = J - J_z$. Here we assume that we can observe each atom separately and detect transitions with 100% efficiency. In this picture, the spectroscopy of uncorrelated atoms described in the last section can be viewed as follows: Each atom is initially prepared in the $|m_s = -\frac{1}{2}\rangle$ eigenstate. Therefore the initial state of this ensemble is the $|J = N/2, M_J = -N/2\rangle$ Dicke state. Using Ramsey spectroscopy on this state results in a precision in spectroscopy characterized by $\Delta\omega = T^{-1}N^{-1/2}$, where T is the Ramsey free precession period [35]. This precision can be understood in terms of the uncertainty of the spin components perpendicular to the mean spin vector for the $|N/2, -N/2\rangle$ Dicke state [35].

For a more general state of mean spin vector $\langle\boldsymbol{J}\rangle$, let $\boldsymbol{J}_\perp$ denote a spin operator perpendicular to $\langle\boldsymbol{J}\rangle$ whose direction is chosen to minimize $\Delta\boldsymbol{J}_\perp$. This state can be used to improve the precision of a frequency measurement in Ramsey spectroscopy over that obtained with the $|J = N/2, -N/2\rangle$ Dicke state discussed above if $\xi_R \equiv \Delta\omega(\text{new state})/\Delta\omega(|J, -J\rangle \text{ Dicke state}) = (2J)^{1/2}\Delta J_\perp/|\langle\boldsymbol{J}\rangle| < 1$ [35]. States with $\xi_R < 1$ correspond to correlated or entangled

atomic states. Methods of generating these states with trapped ions by coupling the internal atomic states to the center-of-mass motion of the ions have been discussed theoretically [35].

We have also considered the possibility of using operators $\tilde{O}$ other than J_z for detection. For $J = N/2$, by measuring J_z it is possible to measure any operator that commutes with J^2 and J_z (that is, any operator diagonal in the $|J, M_J\rangle$ basis). By detecting operators which have higher-order tensor components, states can be used in Ramsey spectroscopy which have $\langle \boldsymbol{J} \rangle = 0$. Using this measurement strategy, we have found states which give $\xi_R = N^{-1/2}$. These states were arrived at through the following reasoning: Referring to the discussion of Ramsey spectroscopy given in Ref. [35], assume that we can prepare the initial state of the system $\psi(0)$ so that after the first $\pi/2$ Ramsey pulse, which rotates J about the $\hat{y}$ axis (in a frame which rotates with the applied radiation [35]), the wave function is given by $\psi(t = t_{\pi/2}) = (|J, +J\rangle + |J, -J\rangle)/2^{1/2}$. After the Ramsey free precession period T, the wave function is given by

$$\psi(t = t_{\pi/2} + T) = [\exp(-i(N/2)(\omega_0 - \omega)T]\,|J, +J\rangle + \exp[i(N/2)(\omega_0 - \omega)T]\,|J, -J\rangle]/2^{1/2},$$

where ω_0 is the spin precession frequency (two-level resonance frequency). This state appears to be the most interesting because the relative phase difference between the two components of the wave function (which can be used to establish an interference signal) is the largest possible. After the second $\pi/2$ Ramsey pulse is applied, the final wave function is given by

$$\psi(t_{\pi/2} + T + t_{\pi/2}) = \psi(t_f) = \exp[i(\pi/2)J_y]\psi(t_{\pi/2} + T).$$

If we assume the signal is given by detecting the operator

$$\tilde{O} \equiv \prod_{i=1}^{N} \sigma_{zi},$$

we find $\Delta\omega = (NT)^{-1}$ and $\xi_R = N^{-1/2}$ for all N.

4. Nonclassical properties of fluorescence radiation from trapped ions

4.1. *Antibunching*

Nonclassical radiation may be studied by measuring the statistics of detected photons. One way to characterize the statistics is through the second-order correlation function $g^{(2)}(t)$ which is defined as the probability of observing a second photon at time t if a photon has been detected at time $t = 0$. For thermal and incoherent fields $g^{(2)}(t)$ is a maximum at $t = 0$ and decreases for larger t [36]. Certain nonclassical or quantum fields exhibit antibunching where $g^{(2)}(t)$ is a minimum for $t = 0$ and initially increases for larger t. The fluorescence from a single atom or trapped ion can show maximum antibunching since $g^{(2)}(0) = 0$. This is so because, if a fluorescent photon is detected at $t = 0$, it takes a while for the atom to be re-excited to the decaying state before it can emit another photon. This effect was first observed for atoms in atomic beams [37, 38]. One or a few ions can be localized in an ion trap; this eliminates the fluctuations in the photon statistics caused by the fluctuating number of atoms in the experimental region in an atomic beam experiment. The first experiments using trapped ions were performed by Diedrich and Walther [39] on an essentially two-level system provided by single $^{24}Mg^+$ ions. More recently, antibunching from a single ion with a multilevel configuration has been reported [40]. In Sec. 3.2, we discussed an observation of antibunching as detected from the statistics of quantum jumps. In this experiment the detector of fluorescent photons is the atom itself (as inferred from the quantum jumps in fluorescence from another transition) as opposed to an external photon detector.

4.2. *Sub-Poissonian statistics*

Sub-Poissonian statistics are also exhibited by fluorescent photons from one or a few trapped ions and atoms. This effect, distinct from antibunching, is characterized by a probability distribution of the number of photons detected in successive time intervals t which is narrower than Poissonian. Although atomic beam experiments have shown antibunching, sub-Poissonian statistics are more difficult to observe [41] because the number of atoms in the observation region fluctuates. This source of fluctuations is absent in the ion experiments. Mandel's Q parameter [42], which can be used to measure the deviation of the distribution from Poissonian statistics, is given by $Q \equiv (\sigma^2 - \langle n \rangle)/\langle n \rangle$ where n is the photon number operator and $\sigma^2 \equiv \langle n^2 \rangle - \langle n \rangle^2$. In the experiments which detect the fluorescent photons directly, Q values of -2.52×10^{-3} [41], -7×10^{-5} [39], and -6×10^{-4} [40] were reported. In the experiment that used the atom's quantum jumps to detect photons [25], a value of -0.253 was reported. The much larger magnitude of Q was due to the nearly unit detection efficiency provided by the quantum jumps.

4.3. *Squeezed light*

Although predicted some time ago [43], squeezing of fluorescent light from single two-level atoms has not been observed yet. Such effects should be observable for ions in traps [44–46] including higher order effects [45].

4.4. *Cavity QED*

The study of the interaction of one or a few atoms with a single mode of the radiation field has been carried out on neutral atoms for a number of years [47]. In optical cavity-QED experiments it would be very desirable to be able to confine a single atom to the Lamb–Dicke limit (spatial excursions $< \lambda/2\pi$). This has been accomplished for ions in a number of experiments and may eventually provide a means for studying cavity-QED effects with trapped ions. For many ion species, this may require high-finesse mirrors in the ultraviolet region of the spectrum.

4.5. *Super- and sub-radiance*

If two atoms are located within about one wavelength of one another, the radiative decay at this wavelength should exhibit the effects of super- and sub-radiance [48]. Two ions bound in a very strong trap might allow observation of these effects under controlled conditions [49].

5. Nonclassical states of particle motion

5.1. *Observation of quantized particle motion*

The limit of cooling for a confined particle is the zero point of motion. For an atomic particle which is (approximately)

harmonically bound, the energy spectrum of eigenstates is given (in one dimension) by $E_n = (n_v + \frac{1}{2})\hbar\omega_v$, where n_v is the vibrational quantum number, and ω_v is the oscillation frequency. The cooling limit is therefore given by $\langle n_v \rangle = 0$. The condition $\langle n_v \rangle \leqslant 1$ has been realized in some ion and neutral atom experiments [50–53]. The value of $\langle n_v \rangle \simeq 0.05$ reported in Ref. [50] showed that the ion was found in the ground state 95% of the time.

For $\langle n_v \rangle \to 0$ the particle motion exhibits nonclassical features. At the limit $\langle n_v \rangle = 0$, the ion motion has finite extent given by the zero-point spread: $\langle x \rangle = 0$, but $(\Delta x)^2 \equiv \langle x^2 \rangle - \langle x \rangle^2 = x_0^2$ where $x_0 = (\hbar/2m\omega_v)^{1/2}$and m is the ion mass. In contrast, for classical motion, cooling can proceed until $\Delta x = 0$. At the cooling limit, the absorption spectrum of a single atom (ion) shows distinct differences between the classical and the quantum mechanical cases. This is revealed in the spectrum of the Doppler-induced frequency-modulation sidebands in the absorption spectrum of a single ion. Classically, the absorption spectrum should show no sidebands at the cooling limit because the velocity approaches zero. Quantum mechanically, at the zero-point energy, the lower absorption sideband, corresponding to the excitation of the ions' internal level accompanied by the reduction of the harmonic oscillator energy by $\hbar\omega_v$, is also absent (the particle motional energy cannot be reduced further). However the upper sideband is always present (the particle motion energy can always be increased). This asymmetry of upper and lower motional sidebands can be used to accurately determine $\langle n_v \rangle$ after cooling is applied [50–53] as illustrated in Fig. 4.

The zero-point motion corresponds to the zero amplitude coherent state or the $n_v = 0$ Fock state. In general, it would be interesting to generate nonclassical states of particle motion, such as squeezed states or perhaps $n_v \neq 0$ Fock states. This has been discussed theoretically in several publications [54–61] and is the subject of the presentations by R. Blatt and P. Toschek at this conference. These studies complement the considerable work that has been devoted to observing nonclassical states of the radiation field [47]. Formally, the problems are similar; however they involve quite different physical systems. In quantum optics, we are concerned with the harmonic oscillators associated with single modes of the radiation field; in the case of trapped ions (or neutral atoms) the harmonic oscillator is associated with the bound motion. In addition to the intrinsic interest in generating such states, they may also be a starting point for other applications. For example, a parametric coupling of ion motion (which has been squeezed) to the internal states of the ions should lead to correlated internal states which can improve the signal-to-noise ratio in spectroscopy [35] (see Section 3.4.2).

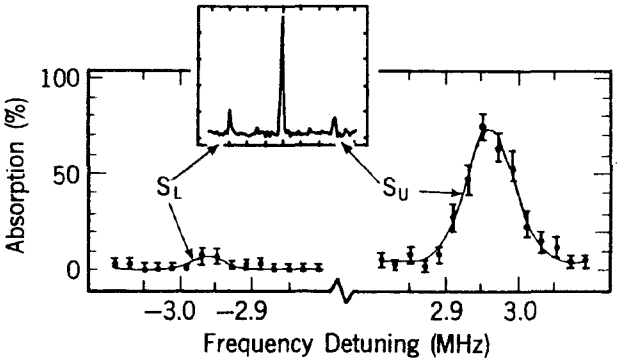

Fig. 4. Absorption spectrum for the $^2S_{1/2} \to {}^2D_{5/2}$ transition in $^{198}Hg^+$. This spectrum is taken the same way as described in Fig. 3 except here, we plot $^2S_{1/2} \to {}^2D_{5/2}$ absorption probability (rather than the probability of not absorbing as in Fig. 3), and we concentrate on the first lower and upper Doppler-shift-induced frequency-modulation sidebands in the spectrum. The inset spectrum was taken before sideband cooling was applied. It shows the carrier at zero detuning and the lower and upper sidebands. The main part of the figure shows the lower (L) and upper (U) sidebands after sideband cooling is applied. This asymmetry in the sideband strengths indicated cooling to the zero-point of quantum mechanical motion about 95% of the time (from Ref. [50]).

5.2. *The Jaynes–Cummings model for trapped ions*

A single two-level system coupled to a single harmonic oscillator is one of the fundamental systems of quantum mechanics. In its simplest form it describes the exchange of quanta between the two-level system and the harmonic oscillator. This model has been studied in considerable detail in the context of quantum optics, where the harmonic oscillator is associated with a single mode of the radiation field; it is usually called the Jaynes–Cummings model [62]. For trapped ions, the harmonic oscillator is associated with the particle motion. A Jaynes–Cummings type of interaction has already been realized to couple the spin and cyclotron motion of a single electron in the classic electron $g - 2$ experiments of Dehmelt and his collaborators [3]. Other realizations of the Jaynes–Cummings model for atomic ions have been considered theoretically. Coupling provided by inhomogeneous magnetic fields (similar to the case realized in electron $g - 2$) have been considered in Refs [35, 63]. Blockley, Walls, and Risken [64] have shown that the Jaynes–Cummings model is realized for a harmonically bound atom or ion which interacts with a traveling wave laser tuned near the transition frequency of the atom. Cirac *et al.* [59] have shown that the Jaynes–Cummings model is realized for the harmonic motion of a two-level ion confined to the Lamb-Dicke limit whose mean position is located at the node of a standing wave laser field tuned near the ion's transition frequency. Reference [35] considered the use of stimulated Raman transitions for the realization of the Jaynes–Cummings model. Because of the relatively weak coupling of the ion motion to the surrounding environment, it should be possible to realize the Jaynes–Cummings model in the limit of small relaxation. One application of the Jaynes–Cummings model coupling is to produce quantum mechanically correlated states between particles for improved spectroscopy [35]. In a similar spirit, it should also be possible to study the dynamics between two coupled quantum mechanical harmonic oscillators [55].

6. Other ion experiments which reveal quantum effects in measurements

Other experiments using stored ions have revealed various quantum mechanical effects of measurement. The interference of the light scattered from two ions (Young's slit experiment where the slits are replaced by two atoms) has been used as demonstration of complementarity without invoking the position-momentum uncertainty relation [65]. An extension of this experiment to the detection of nonclassical features in the fourth-order interference (interference

patterns in the relative positions of simultaneously detected photons in two-photon, two-atom scattering) should be possible [66]. Searches for nonlinear effects in quantum mechanics have been made on both ions and neutral atoms [67]. In situations where large numbers of ions can be viewed as plasmas, it may be possible to achieve a quantized plasma characterized by $\hbar\omega_p > k_B T$, where ω_p is the plasma frequency and k_B is Boltzmann's constant [68].

7. Summary

The long storage times, high degree of spatial localization, and ability to observe individual ions with high detection sensitivity, has allowed the observation of several quantum-mechanical effects in measurements on trapped atomic ions. Some of these observations are facilitated by monitoring fluorescence from an allowed transition in an atomic ion and using discrete changes in this fluorescence as an indicator of changes to other internal states (quantum jumps). This has been applied to the measurement of metastable lifetimes, atomic ion spectra, and observation of quantum mechanical effects such as antibunching of light, the quantum Zeno effect, and quantum projection noise. The fluorescent light from a single, or a few stored ions, shows nonclassical features such as antibunching and sub-Poissonian statistics. The detection of harmonic-motion-induced Doppler sidebands in spectra can reveal quantum mechanical effects in the ion motion. Future possibilities include the observation of squeezed light from single ions, the observation of super- and sub-radiance for 2 or more trapped ions, the generation of nonclassical states of ion motion such as squeezed states, the realization of the Jaynes-Cummings model between atomic ion internal states and ion motion, and the generation of correlated quantum mechanical states for ensembles of atomic ions.

Acknowledgements

We gratefully acknowledge the support of U.S. Office of Naval Research (ONR). We thank D. Meekhof, M. Rauner, and M. Young for helpful comments on the manuscript.

References

1. Schrödinger, E., Br. J. Phil. Sci. III **10**, 109 (1952).
2. Wineland, D., Ekstrom, P. and Dehmelt, H., Phys. Rev. Lett. **31**, 1279 (1973).
3. Dehmelt, H., Science **247**, 539 (1990).
4. Neuhauser, W., Hohenstatt, M., Toschek, P. E. and Dehmelt, H. G., Phys. Rev. **A22**, 1137 (1980).
5. Wineland, D. J. and Itano, W. M., Phys. Lett. **82A**, 75 (1981).
6. Ballentine, L. E., "Quantum Mechanics" (Prentice Hall, NJ 1990), p. 171.
7. Itano, W. M. *et al.*, Phys. Rev. **A47**, 3554 (1993).
8. Bohr, N., Phil. Mag. **26**, 1, 256 (1913).
9. Dehmelt, H. G., Bull. Am. Phys. Soc. **20**, 60 (1975); Dehmelt, H. G., J. Phys. (Paris) (Colloq.) **42**, C8-299 (1981).
10. Cook, R. J. and Kimble, H. J., Phys. Rev. Lett. **54**, 1023 (1985).
11. Blatt, R. and Zoller, P., Eur. J. Phys. **9**, 250 (1988).
12. Erber, T., Hammerling, P., Hockney, G., Porrati, M. and Putterman, S., Ann, Phys. (USA) **190**, 254 (1989).
13. Cook, R. J., in "Progress in Optics, XXVIII" (Edited by E. Wolf) (North Holland, Amsterdam 1990), p. 361.
14. Cohen-Tannoudji, C. and Dalibard, J., Europhys, Lett. **1**, 441 (1986).
15. Nagourney, W., Sandberg, J. and Dehmelt, H. G., Phys. Rev. Lett. **56**, 2797 (1986).
16. Sauter, Th., Blatt, R., Neuhauser, W. and Toschek, P. E., Phys. Rev. Lett. **57**, 1696 (1986).
17. Bergquist, J. C., Hulet, R. G., Itano, W. M. and Wineland, D. J., Phys. Rev. Lett. **57**, 1699 (1986).
18. Madej, A. A. and Sankey, J. D., Phys. Rev. **A41**, 2621 (1990).
19. Itano, W. M., Bergquist, J. C., Hulet, R. G. and Wineland, D. J., Phys. Rev. Lett. **59**, 2732 (1987).
20. Madej, A. A. and Sankey, J. D., Opt. Lett. **15**, 634 (1990).
21. Barwood, G. P., Edwards, C. S., Gill, P., Klein, H. A. and Rowley, W. R. C., in: "Laser Spectroscopy (Proceedings XIth International Conference) (Edited by L. Bloomfield, T. Gallagher and D. J. Larson) (AIP Conf. Proc. 290) (AIP Press, New York 1994), p. 35.
22. Urabe, S., Watanabe, M., Imajo, H. and Hayasaka, K., Opt. Lett. **17**, 1140 (1992).
23. Peik, E., Hollemann, G. and Walther, H., Phys. Rev. **A49**, 402 (1994).
24. Church, D. A., Phys. Rep. **228**(5 & 6), 253 (1993).
25. Itano, W. M., Bergquist, J. C. and Wineland, D. J., Phys. Rev. **A38**, 559 (1988).
26. Cook, R. J., Physica Scripta **T21**, 49 (1988).
27. Itano, W. M., Heinzen, D. J., Bollinger, J. J. and Wineland, D. J., Phys. Rev. **A41**, 2295 (1990). Recent discussions concerning the quantum Zeno effect are summarized in: Itano, W. M., Bergquist, J. C., Bollinger, J. J. and Wineland, D. J., Proc. 20th International Colloq. on Group Theoretical Methods in Physics, Toyonaka, Japan, July, 1994.
28. Peres, A. and Ron, A., Phys. Rev. **A42**, 5720 (1990).
29. Wineland, D. J., Bergquist, J. C., Itano, W. M. and Drullinger, R. E., Opt. Lett. **5**, 245 (1980).
30. Bergquist, J. C., Itano, W. M. and Wineland, D. J., Phys. Rev. **A36**, 428 (1987).
31. Nagourney, W., Yu, N. and Dehmelt, H., Opt. Commun. **79**, 176 (1990).
32. Appasamy, B. *et al.*, submitted to Appl. Phys. B.
33. Madej, A. A., Siemsen, K. J., Sankey, J. D., Clark, R. F. and Vanier, J., IEEE Trans. Instrum. Meas. **42**, 234 (1993).
34. Barwood, G. P., Edwards, C. S., Gill, P., Klein, H. A. and Rowley, W. R. C., Opt. Lett. **18**, 732 (1993).
35. Wineland, D. J., Bollinger, J. J., Itano, W. M., Moore, F. L. and Heinzen, D. J., Phys. Rev. **A46**, R6797 (1992); Wineland, D. J., Bollinger, J. J., Itano, W. M. and Heinzen, D. J., Phys. Rev. **A50**, 67 (1994).
36. Hanbury Brown, R. and Twiss, R. Q., Nature **177**, 27 (1956); **178**, 1447 (1956).
37. Kimble, H. J., Dagenais, M. and Mandel, L., Phys. Rev. Lett. **39**, 691 (1977); Dagenais, M. and Mandel, L., Phys. Rev. **A18**, 2217 (1978).
38. Rateike, F.-M., Leuchs, G. and Walther, H. (results cited by Cresser, J. D., Häger, J., Leuchs, G., Rateike, F.-M. and Walther, H., in: "Dissipative Systems in Quantum Optics" (Topics in Current Physics, Vol. 27) (Edited by R. Bonifacio) (Springer, Berlin 1982), p. 21.
39. Diedrich, F. and Walther, H., Phys. Rev. Lett. **58**, 203 (1987).
40. Schubert, M., Siemers, I., Blatt, R., Neuhauser, W. and Toschek, P. E., Phys. Rev. Lett. **68**, 3016 (1992).
41. Short, R. and Mandel, L., Phys. Rev. Lett. **51**, 384 (1983).
42. Mandel, L., Opt. Lett. **4**, 205 (1979).
43. Walls, D. F. and Zoller, P., Phys. Rev. Lett. **47**, 709 (1981).
44. Vogel, W. and Welsch, D.-G., Phys. Rev. Lett. **54**, 1802 (1985).
45. Vogel, W., Phys. Rev. Lett. **67**, 2450 (1991).
46. Vogel, W. and Blatt, R., Phys. Rev. **A45**, 3319 (1992).
47. See, for example, the reviews in "Fundamental Systems in Quantum Optics" (Edited by J. Dalibard, J. M. Raimond, and J. Zinn-Justin, Les Houches, Session LIII) (North Holland, Amsterdam 1992).
48. Dicke, R. H., Phys. Rev. **93**, 99 (1954).
49. Devoe, R. G. and Brewer, R. G., Bull. Am. Phys. Soc. **38**, 1140 (1993).
50. Diedrich, F., Bergquist, J. C., Itano, W. M. and Wineland, D. J., Phys. Rev. Lett. **62**, 403 (1989).
51. Verkerk, P. *et al.*, Phys. Rev. Lett. **68**. 3861 (1992).
52. Jessen, P. S. *et al.*, Phys. Rev. Lett. **69**, 49 (1992).
53. Hemmerich, A. and Hänsch, T. W., Phys. Rev. Lett. **70**, 410 (1993).
54. Bergquist, J. C., Diedrich, F., Itano, W. M. and Wineland, D. J., in "Laser Spectroscopy IX" (Edited by M. S. Feld, J. E. Thomas, and A. Mooradian) (Academic Press, San Diego 1989), p. 274.
55. Heinzen, D. J. and Wineland, D. J., Phys, Rev. **A42**, 2977 (1990).
56. Cirac, J. I., Parkins, A. S., Blatt, R. and Zoller, P., Phys. Rev. Lett. **70**, 556 (1993).

57. Baseia, B., Vyas, R. and Bagnato, V. S., Quantum Opt. **5**, 155 (1993).
58. Zeng. H. and Lin, F., Phys. Rev. **A48**, 2393 (1993).
59. Cirac, J. I., Blatt, R., Parkins, A. S. and Zoller, P., Phys. Rev. Lett. **70**, 762 (1993).
60. Cirac, J. I., Blatt, R. and Zoller, P., Phys. Rev. **A49**, R3174 (1994).
61. Cirac, J. I., Blatt, R., Parkins, A. S. and Zoller, P., Phys. Rev. **A49**, 1202 (1994).
62. Jaynes, E. T. and Cummings, C. W., Proc. IEEE **51**, 89 (1963).
63. Harde, H., in "International Conference on Quantum Electronics Technical Digest Series *1990*", Vol. 8) (Optical Society of America, Washington, DC 1990), p. 278.
64. Blockley, C. A., Walls, D. F. and Risken, H., Europhys. Lett. **17**, 509 (1992).
65. Eichmann, U. *et al.*, Phys. Rev. Lett. **70**, 2359 (1993).
66. Itano, W. M. *et al.*, "Lasers '93" (Proceedings of the International Conference, Lake Tahoe, NV, Dec. 1993, Society for Optical and Quantum Electronics) (STS Press, McLean, VA 1994), p. 412.
67. Bollinger, J. J., Heinzen, D. J., Itano, W. M., Gilbert, S. L. and Wineland, D. J., in "Atomic Physics 12" (Proceedings of the 12th International Conference on Atomic Physics) (Edited by J. C. Zorn and R. R. Lewis) (American Institute of Physics Press, New York 1991), p. 461.
68. Wineland, D. J., Weimer, C. S. and Bollinger, J. J., Hyperfine Interactions **76**, 115 (1993).